Journal of Cell Science 111, 1227-1240 (1998)
Printed in Great Britain © The Company of Biologists Limited 1998
JCS7183

Microtubule-mediated centrosome motility and the positioning of cleavage furrows in multinucleate myosin II-null cells

Ralph Neujahr*, Richard Albrecht, Jana Köhler, Monika Matzner, Jean-Marc Schwartz, Monika Westphal and Günther Gerisch

Max-Planck-Institut für Biochemie, D-82152 Martinsried, Germany
*Author for correspondence

Accepted 17 February; published on WWW 20 April 1998

SUMMARY

To study centrosome motility and the interaction of microtubules with the cell cortex in mitotic, post-mitotic and interphase cells, α-tubulin was tagged in *Dictyostelium discoideum* with green fluorescent protein. Multinucleate cells formed by myosin II-null mutants proved to be especially suited for the analysis of the control of cleavage furrow formation by the microtubule system. After docking of the mitotic apparatus onto the cell cortex during anaphase, the cell surface is activated to form ruffles on top of the asters of microtubules that emanate from the centrosomes. Cleavage furrows are initiated at spaces between the asters independently of the positions of spindles. Once initiated, the furrows expand as deep folds without a continued connection to the microtubule system. Occurrence of unilateral furrows indicates that a closed contractile ring is dispensable for cytokinesis in *Dictyostelium*. The progression of cytokinesis in the multinucleate cells underlines the importance of proteins other than myosin II in specifying a cleavage furrow. The analysis of centrosome motility suggests a major role for a minus-end directed motor protein, probably cytoplasmic dynein, in applying traction forces on guiding microtubules that connect the centrosome with the cell cortex.

Key words: Contractile ring, Cytokinesis, *Dictyostelium discoideum*, Dynein, GFP-tubulin, Motor protein

INTRODUCTION

Mitotic cell division is based on the coordinated activities of the microtubule and microfilament systems. At the commencement of mitosis, the interphase microtubules are replaced by microtubules that build the spindle and others that form asters around the spindle poles. Interaction of the mitotic apparatus with the cortical region of a dividing cell is important for the actin system to form a cleavage furrow at the correct location and exactly after segregation of the chromosomes along the spindle. The cleavage furrow incises the cell body between the asters and eventually separates the daughter cells (for reviews, see Conrad and Schroeder, 1990; Rappaport, 1996). In interphase cells the microtubule system is organized by the centrosomes, which are normally linked to the nucleus and Golgi apparatus.

Two lines of experimentation have provided most of our knowledge on the interaction of the microtubule system with the cortex of a dividing cell. One is the experimental dislocation of the mitotic apparatus, the other is the utilization of a system in which the nucleus and centrosome are naturally translocated from a central position to their proper location in the cortical region of a cell. Classical experiments performed by mechanically dislodging the nucleus have demonstrated that, in dividing sea urchin eggs, cleavage furrows are formed in the space between two asters, and this process is independent of the presence of a spindle (Rappaport, 1961, 1986). The blastoderm formed by nuclear migration and cellularization in early *Drosophila* development is a superior, although specialized, system for the genetical analysis of the organization of the cell cortex in coordination with the underlying system of microtubules (Schejter and Wieschaus, 1993).

In order to analyse the dynamics of microtubule-cortex interactions, we have used multinucleate cells of myosin II–null mutants grown up in suspension (DeLozanne and Spudich, 1987; Knecht and Loomis, 1987) and compared them with wild-type cells of *Dictyostelium discoideum*. Fixed preparations of myosin II-null cells indicated that the mitotic complexes are translocated during anaphase from the center to the cortical region of the cells (Neujahr et al., 1997a). To continuously record microtubule dynamics in living cells, we have tagged α-tubulin from *D. discoideum* with green fluorescent protein (GFP). The fusion protein incorporated into cytoplasmic microtubules and also into the spindle, as has recently been shown for yeast α-tubulin (Carminati and Stearns, 1997; Straight et al., 1997). Two questions will be addressed. How is centrosome motility guided, and how are cleavage and cell-surface ruffling in mitotic cells linked to the microtubule system?

MATERIALS AND METHODS

Vector construction and transformation of *Dictyostelium* cells

Vectors for the expression of a GFP-α-tubulin fusion under the actin 15 promoter were constructed from either the plasmid pDEXRH (Faix et al., 1996) or from pDBsr (kindly obtained from A. Erdmann). The insert in both vectors comprised a continuous reading frame from 5′ to 3′ of the sequence of GFP S65T (Heim and Tsien, 1996), a hexapeptide linker KLGGRQ, which resulted from the cloning procedure, and the entire coding region of a *D. discoideum* α-tubulin cDNA clone (kindly provided by C.-L. Lu and G. Marriott). After introducing cloning sites by PCR, the sequence was verified by comparison with the authentic α-tubulin sequence (Trivinos-Lagos et al., 1993). The entire insert was blunt-end ligated into *Hin*dIII sites. Cells were transfected by electroporation.

The pDEXRH vector construct was used for selection of transformants in the AX2 wild-type strain with 20 μg ml^{-1} of G418, and the pDBsr construct for selection in the G418-resistant myosin II-null mutant with 20 μg ml^{-1} of blasticidin S. HS2205 is a derivative of AX2 obtained by eliminating the myosin II heavy chain through gene replacement (Manstein et al., 1989). The GFP-α-tubulin producing clone from AX2-214 was designated as HG1668, and that from HS2205 as HG1671.

Culture and treatment of GFP-α-tubulin-producing cells

Uninucleate cells were obtained by culture in polystyrene Petri dishes with nutrient medium. To produce multinucleate cells, HG1671 was cultivated for 36 hours in shaken suspension with nutrient medium according to DeLozanne and Spudich (1987) and Knecht and Loomis (1987).

For confocal microscopy, HG1671 cells were gently transferred into a chamber consisting of a 5×5 cm glass coverslip onto which a plastic ring of 40 mm diameter was mounted with paraffin. The chamber was filled with 5 ml of nutrient medium, and the cells were imaged either freely dividing in the fluid layer or under compression by a 0.2 mm layer of agarose (Yumura et al., 1984). For time-lapse microscopy in the experiment shown in Fig. 8, HG1668 cells were incubated in the chamber with 17 mM K/Na-phosphate buffer, pH 6.0, supplemented with *Klebsiella aerogenes* as a food source in order to minimize background fluorescence caused by the nutrient medium. Immediately before microscopy, these cells were strongly compressed by agar overlay (Yumura et al., 1984).

Butanedione monoxime (BDM; Sigma Chemical Co., St Louis, MO 63178, USA) was diluted from a 5 M stock solution in DMSO into 17 mM K/Na-phosphate buffer, pH 6.0. Cells were preincubated for 15 minutes with 50 or 100 mM of the drug, and overlaid with an agarose sheet equilibrated with the same solution before centrosome movement was assessed.

Confocal and time-lapse fluorescence imaging

Confocal fluorescence images were obtained in parallel to phase-contrast images using an LSM 410 microscope and a 100×1.3 Plan NEOFLUAR objective (Zeiss). To minimize damage by light, cells entering mitosis were first identified by conventional phase-contrast microscopy. Subsequently, the 488 nm line of an argon-ion laser was used for excitation. The pinhole was slightly opened, so that confocality was reduced to a resolution of 1.9 μm in the *z*-axis.

For time-lapse microscopy of the GFP S65T fluorescence, an Axiovert microscope (Zeiss) was equipped with an adjustable tungsten lamp. A D485 filter was used for excitation and a Q505 dichroic mirror and a HQ535/50 filter for emission, all purchased from Chroma Technology Corp. (Brattleboro, VT 05301, USA). The emission was recorded using a SIT C 2400-08 camera (Hamamatsu). A frame grabber (MVC-Image Capture PCI, Imaging Technology Incorporation, Bedford, MA 01730, USA) served as a digitizer to transfer the data within less than 20 milliseconds to the memory of a host PC before the data were converted to TIFF format. Software was designed to read the images out of the memory, to adjust frame size, time-lapse interval and number of frames in a series, and to average fluorescence images for noise suppression. One image was obtained per second by averaging over four frames of the SIT camera.

Using Application Visualization System software (Advanced Visual Systems Inc., Waltham, MA 02154, USA), non-linear contrast enhancement was applied on microtubule fluorescence intensities. For Fig. 8, a color table progressing from black to red and yellow was applied.

Electron microscopy

In the flat cortexillin I/II double mutant cells of *D. discoideum* (Faix et al., 1996) the nuclei and centrosomes were mostly located in one plane. Mutant cells spread on glass were fixed for 15 minutes at room temperature followed by 45 minutes on ice in 17 mM K/Na-phosphate buffer, pH 6.0, containing 1% glutaraldehyde and 0.1% osmium tetroxide. After staining for 1 hour on ice with 1% uranyl acetate, the specimens were dehydrated with ethanol and embedded in epon. 70 nm sections were stained with 3% lead citrate and 4% uranyl acetate, and micrographs taken on a JEM 100 CX transmission electron microscope (Joel) on Scienta EM film (AGFA).

RESULTS

Spindle dynamics and cytokinesis in GFP-α-tubulin-labelled wild-type and myosin II-null cells

In order to record microtubule dynamics and centrosome motility in parallel with changes in cell shape, wild-type and myosin II-null cells were transfected with a vector encoding a GFP-α-tubulin fusion protein. In both the wild-type and mutant cells, two activities associated with the actin cytoskeleton in the cell cortex are linked to mitosis. The first activity is displayed by the polar regions of the cell, and is characterized by dynamic protrusions that have the appearance of ruffles. Similar protrusions ultimately form the leading edges of each daughter cell. The second activity is typified by the smooth surface of the rapidly progressing cleavage furrow (Fig. 1, phase contrast images). The midzone of the cell becomes constricted at the end of telophase, when the spindle has already disassembled between the separated daughter nuclei (Fig. 1, fluorescence images). Cleavage proceeds to completion while the microtubule system is being re-organized into the interphase state.

The uninucleate myosin II-null cell shown in Fig. 1B passed through the same stages of cytokinesis but divided more slowly than the wild-type cell in Fig. 1A. This is consistent with the broad variation in time required by myosin II-null cells for cytokinesis (Neujahr et al., 1997a).

Docking of the mitotic apparatus to the cortex in multinucleate cells, followed by cell-surface ruffling and furrowing

Multinucleate myosin II-null cells, generated in suspension and transferred to a glass surface, exhibit surface activities similar to those coupled to mitosis in uninucleate cells (Fig. 2). After docking of the mitotic apparatus (MA) to the cell cortex, cell-surface ruffling is strongly increased (Fig. 2A, 280- compared to 0-second frame). This ruffling is comparable to the activities of the polar regions of uninucleate

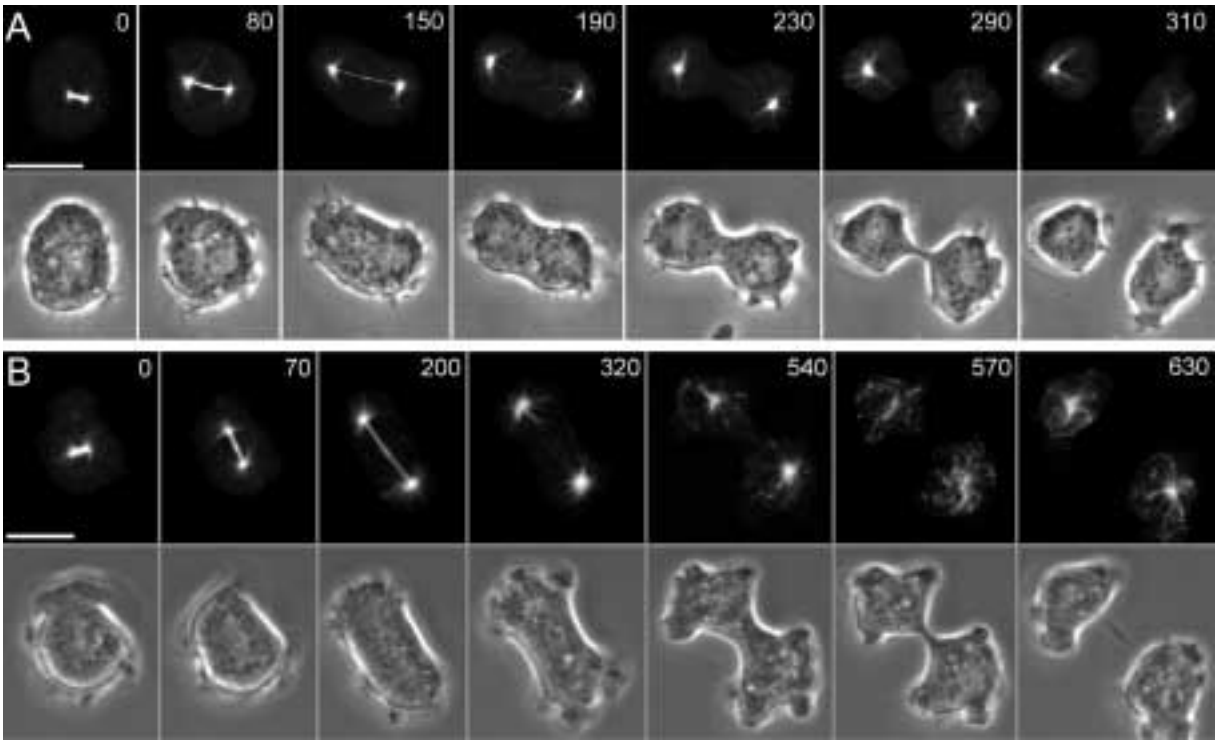

Fig. 1. Microtubule dynamics in mitotic cells aligned with cytokinesis. Wild-type (A) and myosin II-null (B) cells producing GFP-α-tubulin divided in a fluid layer on a glass surface. Numbers indicate seconds after the beginning of each sequence. Overlap of microtubules in the middle region of the spindle is recognizable at the 80- and 70-second frames, respectively, of A and B. In B the spindle rotated and assumed its final orientation at 2 minutes before the position of the cleavage furrow became apparent. Constriction of the cleavage furrow started at the 190-second frame in A, and the 320-second frame in B; this means that it was coincident with disassembly of the spindle in both the wild-type and myosin II-null cell. Fluorescence images (upper panels) were obtained by confocal laser scanning microscopy; the shapes of the same cells are shown in phase contrast (lower panels). Bars, 10 μm.

cells, and is concentrated to cell-surface areas that are underlaid by centrosomes and connected to the microtubule asters emanating from them. The centrosomes are located at the distal side of the nuclei close to the ruffling surface, a position which corresponds to the regular location of centrosomes in motile interphase cells (see the uninucleate cell on top of the multinucleate one in Fig. 2C, 360-second frame). Microtubules arranged in an arrowhead configuration are in fact attached to the nuclear surface (in the 280- and 460-second frames of Fig. 2A). In multinucleate cells cleavage furrows grow out from small, rounded invaginations of the cell surface between the asters (Fig. 2A, 280- to 460-second frames). When furrows fuse, they either cleave the cell into two or more portions containing multiple nuclei, or they give rise to uninucleate buds (Fig. 2A, 780-second frame).

The two cells shown in Fig. 2B,C illustrate special features of cytokinesis in multinucleate cells. The cell in Fig. 2B exemplifies unilateral progression of a cleavage furrow. This furrow spreads over the entire lower surface of the cell, and at one point meets with a furrow incising the cell from above. Fusion of the two furrows results in cleavage of the cell (filled arrowhead in Fig. 2B, 340-second frame). A third furrow formed in this cell stops growing but persists as an irregularly folded part of the cell surface (open arrowhead).

In the cell shown in Fig. 2C, docking of the asters results in bending of the spindles, as previously observed in fixed preparations of cells not transfected with a GFP-α-tubulin fusion construct (Neujahr et al., 1997a). Since a spindle is formed in *Dictyostelium* by 20 or more microtubules emanating from each spindle pole body (Moens, 1976; McIntosh et al., 1985), the forces generated by docking of the asters to the cell cortex must be strong enough to overcome the combined stiffness of that number of microtubules.

At the stage of docking the cell surface is still smooth, indicating that docking precedes the ruffling period. Subsequently, protrusions are profusely formed over the surface of the cell shown in Fig. 2C (980-second frame). The abundance of protrusions is probably due to the decreased surface to volume ratio of this exceptionally large cell. As a consequence, the microtubule asters become densely packed and capable of imprinting ruffling activity onto the entire cell surface. It is only at a late stage that a single cleavage furrow is formed in this cell (Fig. 2C, 1560-second frame).

Fig. 3 illustrates the spatial relationship between the positions of asters and cleavage furrows that are initiated between them. In the binucleate wild-type cell shown in Fig. 3A, furrows are formed between each aster of microtubules, regardless of whether or not they are connected by a spindle. Similarly, in multinucleate myosin II-null cells, cleavage furrows often arise at sites between two asters that are connected to each other via the spindle, but they can also be formed at the interspace between separate mitotic complexes

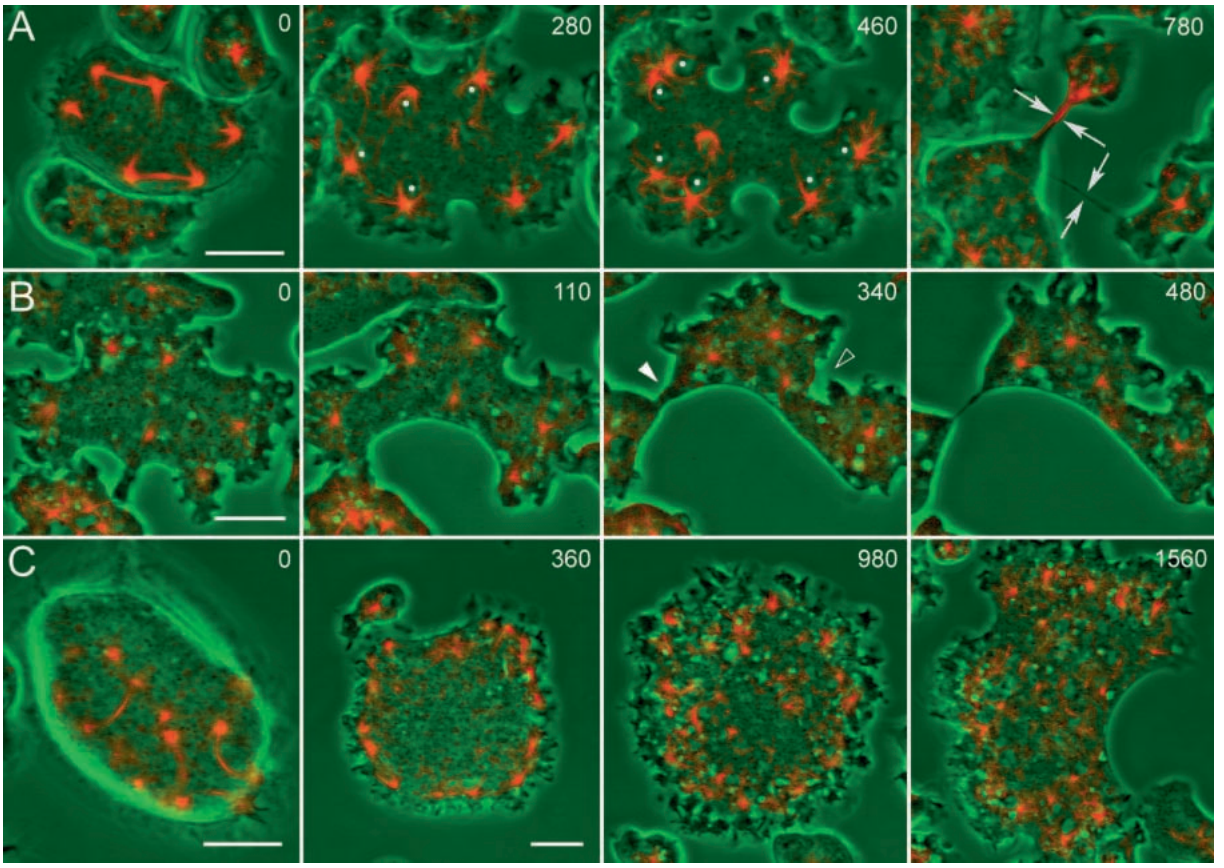

Fig. 2. Three cells exemplifying cytokinesis in multinucleate myosin II-null cells. To relate microtubule dynamics to changes in cell shape and cleavage, confocal GFP-α-tubulin fluorescence images are falsely coloured in red and superimposed onto simultaneously recorded phase-contrast images displayed in green. (A) Formation of multiple cleavage furrows, which were sharply separated from the ruffled areas of the cell surface. In the 280- and 460-second frames centrosomes were located beneath the ruffling areas, typically at the distal side of the nuclei, whose centers are marked by white dots. The furrow in the middle fused with the two other ones, as indicated in the 780-second frame by arrows. The three daughter cells became completely separated from each other at 180 seconds later. (B) Unilateral furrow formation. A large furrow derived from two separate furrows on the lower cell surface. From above, a progressing and an abortive furrow were produced. The small furrow on the left side of the upper surface (filled arrowhead in the 340-second frame) led to complete cleavage at 220 seconds after the 480-second frame. The furrow on the upper right lost its rounded surface (open arrowhead in the 340-second frame) but persisted as an indentation for at least 11 minutes after the end of the sequence. (C) A large cell showing that docking of asters to the cell cortex precedes cell-surface ruffling. Ruffling then continued most extensively at the surface of this unusually big cell after the centrosomes had left their initial sites of docking (980-second frame). A furrow appeared late at the right hand side of the cell. In the 360-second image a cell entered the field of view, which revealed the typical centrosome location in an interphase cell behind the leading edge and in front of the nucleus. The cells in A and C divided in a fluid layer on a glass surface, that in B was slightly compressed by agar overlay. Bars, 10 μm; the bar on the 360-second frame in C also applies to the subsequent frames.

(arrowheads in Fig. 3B). The centrosomes do not rest at their initial sites of docking. They move apart not only during the lengthening of spindles, but also after breakdown of the cytoplasmic portions of the spindles (Fig. 3, centrosomes numbered 1 to 3). While the centrosomes thus separate from their docking sites, the cleavage furrows, once primed, proceed to incise the cell body, increasing in area until they encounter an opposing furrow.

Because of irregularities in the initiation, progression or fusion of cleavage furrows in multinucleate myosin II-null cells, cleavage products strongly vary in size. Fig. 4A illustrates an extreme example of unequal division. Of interest is the unusually small daughter cell boxed in the 800-second panel. In this cell, the centrosome circulated together with the complement of microtubules for more than 13 minutes, with the centrosome in front and the bulk of microtubules forming a tail (Fig. 4B). The average time required for one rotation was 45 seconds. This circular movement of a centrosome was repeatedly observed in small uninucleate cells produced by the budding of large myosin II-null cells. It was not due to rotation of the entire cell, as judged from stationary vesicles recognizable in phase contrast.

Guiding microtubules interacting with the cell cortex in mitotic cells

Centrosome movement is most evident in multinucleate cells, but it reflects an activity also found in normal, uninucleate cells. In order to analyse this motility, we have imaged

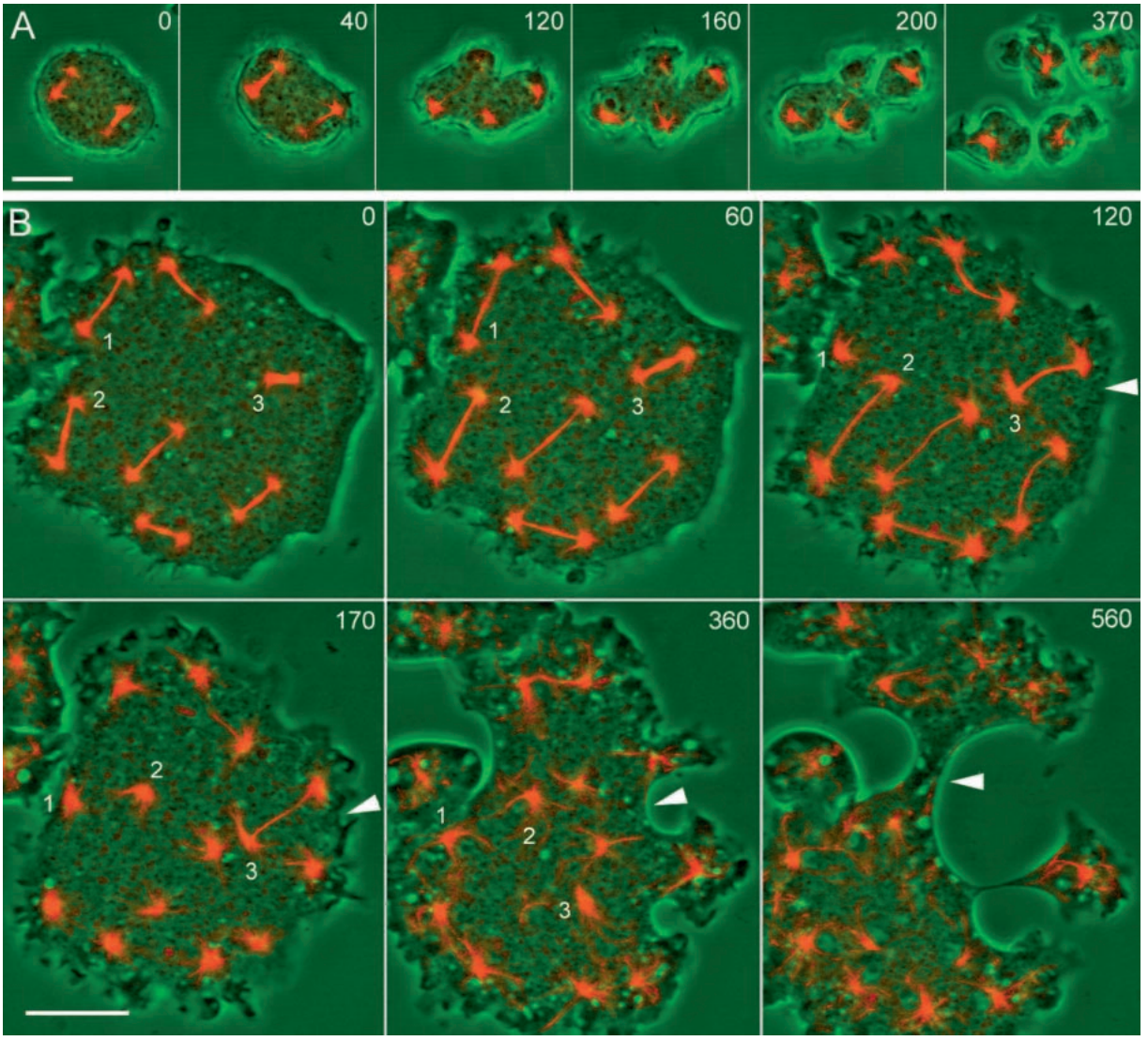

Fig. 3. A binucleate wild-type cell (A) and a multinucleate myosin II-null cell (B) showing similar positioning of cleavage furrows. The wild-type cell divided uncompressed as did the uninucleate cells shown in Fig. 1. The myosin II-null cell was strongly compressed so that asters docked to the upper or lower cell surface are seen in one plane. In both cells, furrows formed in the spaces between mitotic complexes as well as on top of the spindles. In A the furrows separating the two mitotic complexes even preceded the other ones. In B a furrow formed between asters that belonged to separate mitotic complexes is marked by the arrowhead. In this cell, cleavage is clearly seen to proceed while centrosomes leave their initial sites of docking. The changing positions of three centrosomes are indicated by numbers. Fluorescence is superimposed onto phase-contrast images as in Fig. 2. Numbers are seconds after the first frame. Bars, 10 μm.

uninucleate wild-type and myosin II-null cells with high resolution at mitotic, post-mitotic and interphase stages.

Fig. 5 shows how centrosomes interact, from the anaphase onwards, with the cell cortex by the extension of microtubules. Often single microtubules or thin bundles span the gap to the cortex in the direction of the centrosome's movement. We designate these microtubules 'guiding microtubules', to distinguish them from the majority of microtubules in an aster, which trail behind the moving centrosomes. Microtubules exert the guiding function only temporarily, as indicated by the examples shown in Fig. 5A,C,D.

Stage by stage comparison of wild-type (Fig. 5A,B) and myosin II-null cells (Fig. 5C-E) indicates that interactions of the MA with the cell cortex are evidently not altered by the absence of the motor protein. The interval between the 0- and 20-second frames of Fig. 5C demarcates the mitotic stage at which microtubular connections between the centrosomes and the cell cortex become detectable. At the beginning, long microtubules are protruded from the centrosomes towards the cell cortex (Fig. 5A, 0-frame). Subsequently, the distance between centrosomes and cell periphery is shortened, often under rotation of the spindle (Fig. 5C). This process is comparable to the docking of the MAs in multinucleate cells, which occurs at the same mitotic stage (Fig. 4A, 60-second frame).

Spindle bending, as observed at telophase stages of multinucleate cells (Fig. 2C, 0-frame), also occurs in uninucleate

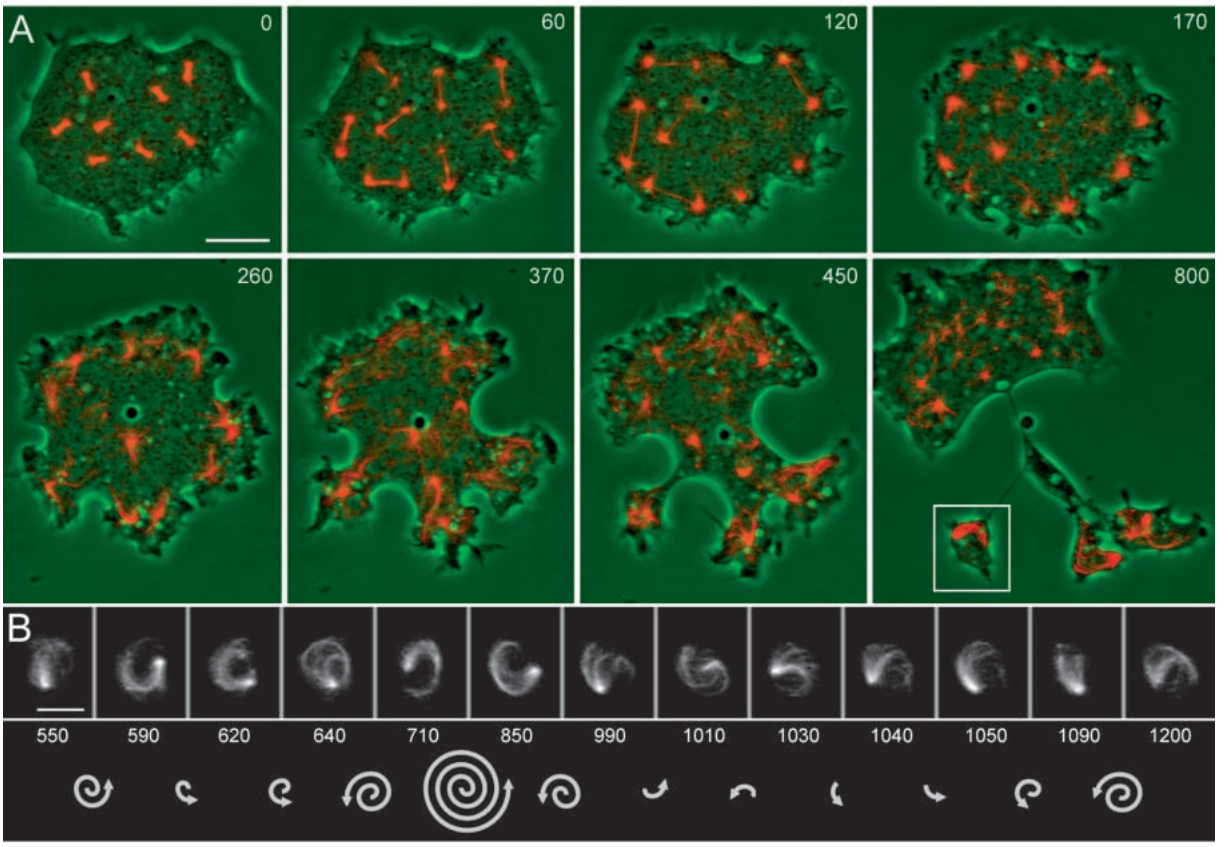

Fig. 4. Unequal division of a multinucleate myosin II-null cell followed by circular movement of the microtubule system in a small post-mitotic cell. (A) After typical anaphase docking of microtubule systems (0- to 120-second panels) and membrane ruffling above the asters (120- to 170-second panels), this cell gave rise to three daughter cells of extremely different sizes. An unusually small uninucleate cell is boxed in the last frame. The cell was slightly flattened by an agar overlay and imaged as in the previous figures. (B) Circulation of the centrosome with a comet-like tail of microtubules in the cell boxed in A. The top row shows GFP-α-tubulin fluorescence, the bottom indicates the number of circles passed between the frames. Numbers are seconds after the first frame in A. Bars, 10 μm (A), 5 μm (B).

cells, as shown in the telophase sequences of Fig. 5A,D. Fig. 5A illustrates the microtubule dynamics linked to spindle bending. Between the 80- and 90-second frames the centrosome on the left side is laterally connected to the cell cortex by what appears to be a bundle of microtubules, as judged from its high fluorescence intensity. This microtubular bridge is moved along the cell cortex towards the top of the images. As a consequence, the spindle is bent into a U-turn (Fig. 5A, 110-second frame). Straightening of the spindle coincides with the switch to other microtubules that extend from the centrosome to the opposite side of the cell (Fig. 5D, 70-second frame).

At the end of telophase, the two centrosomes still connected by the spindle move preferentially into opposite directions, as demonstrated in the multinucleate cell shown in Fig. 3. Accordingly, guiding microtubules contact the cell cortex roughly in the direction of the spindle (Fig. 5B,E). These microtubules are clearly distinguishable from the microtubules that surround the nucleus behind the centrosome in an arrowhead configuration.

Centrosome movement in post-mitotic cells and passive translocation of the nuclei

In electron micrographs the centrosome is typically attached to a tipped extension of the nuclear envelope (Fig. 6A). Microtubules make contact with the nucleus near to their origin at the centrosome and also further along their length. Fig. 6B shows a compact intranuclear bundle of microtubules connected to the centrosome, which corresponds to a remnant of the spindle often seen to traverse the nucleus at the post-mitotic stage. In living cells, this intranuclear remnant of the spindle proved to be a valuable indicator of the position and translocation of the nucleus.

Only few microtubules emanate from a centrosome at the post-mitotic stage, and they have not yet attained their full length. In cells with this incomplete complement of microtubules, phases of more or less straight movement of centrosomes typically alternated with abrupt changes in direction (Fig. 7A). During the straight runs of this saltatory type of movement, velocities varied between 0.2 and 0.7 μm per second, with an average of 0.35 μm per second, based on 11 independent series of post-mitotic myosin II-null cells. Often guiding microtubules were seen to point during these phases into the direction of the centrosome movement (Fig. 7B).

The intranuclear remnant of the spindle was used to identify the organelle at which the forces responsible for the joint

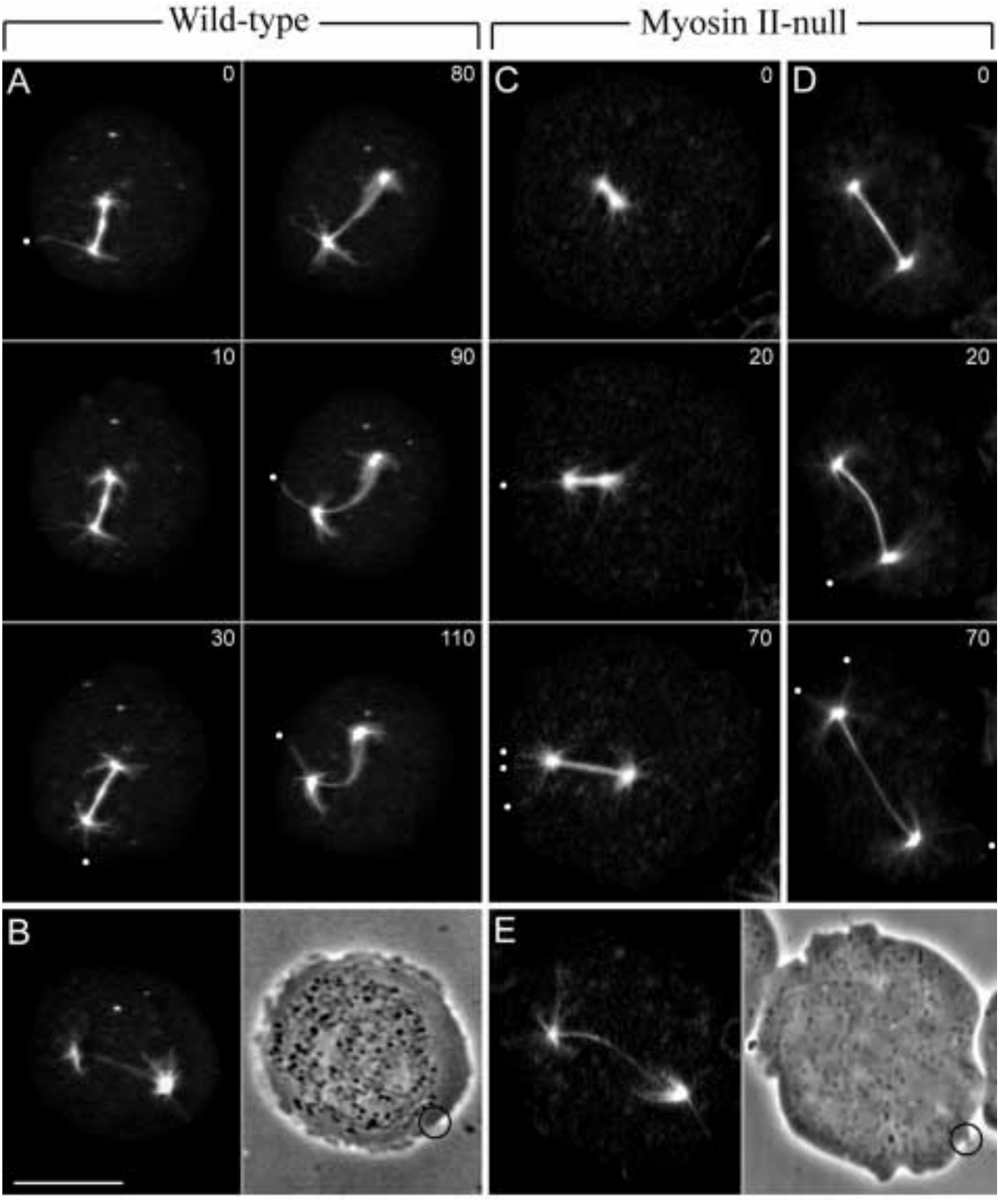

Fig. 5. Dynamics of microtubule interactions with the cell cortex in mitotic cells. Mitotic stages of wild-type AX2 cells (A,B) are compared with those of uninucleate myosin II-null cells (C-E). Cells were strongly compressed by an agar overlay in order to follow microtubules by confocal scanning microscopy over their entire length. (A,C,D) Anaphase and telophase stages. Sites of microtubule interaction with the cell cortex are marked by white dots. Numbers are seconds after the beginning of each sequence. (B,E) Fluorescence (left panels) and phase-contrast (right panels) images of post-telophase stages. Each cell shows on its right-hand centrosome a single microtubule (or thin bundle) that is separate from the majority of microtubules in the aster, and which makes contact with the cortex at the positions encircled in the phase-contrast images. Bar, 10 μm.

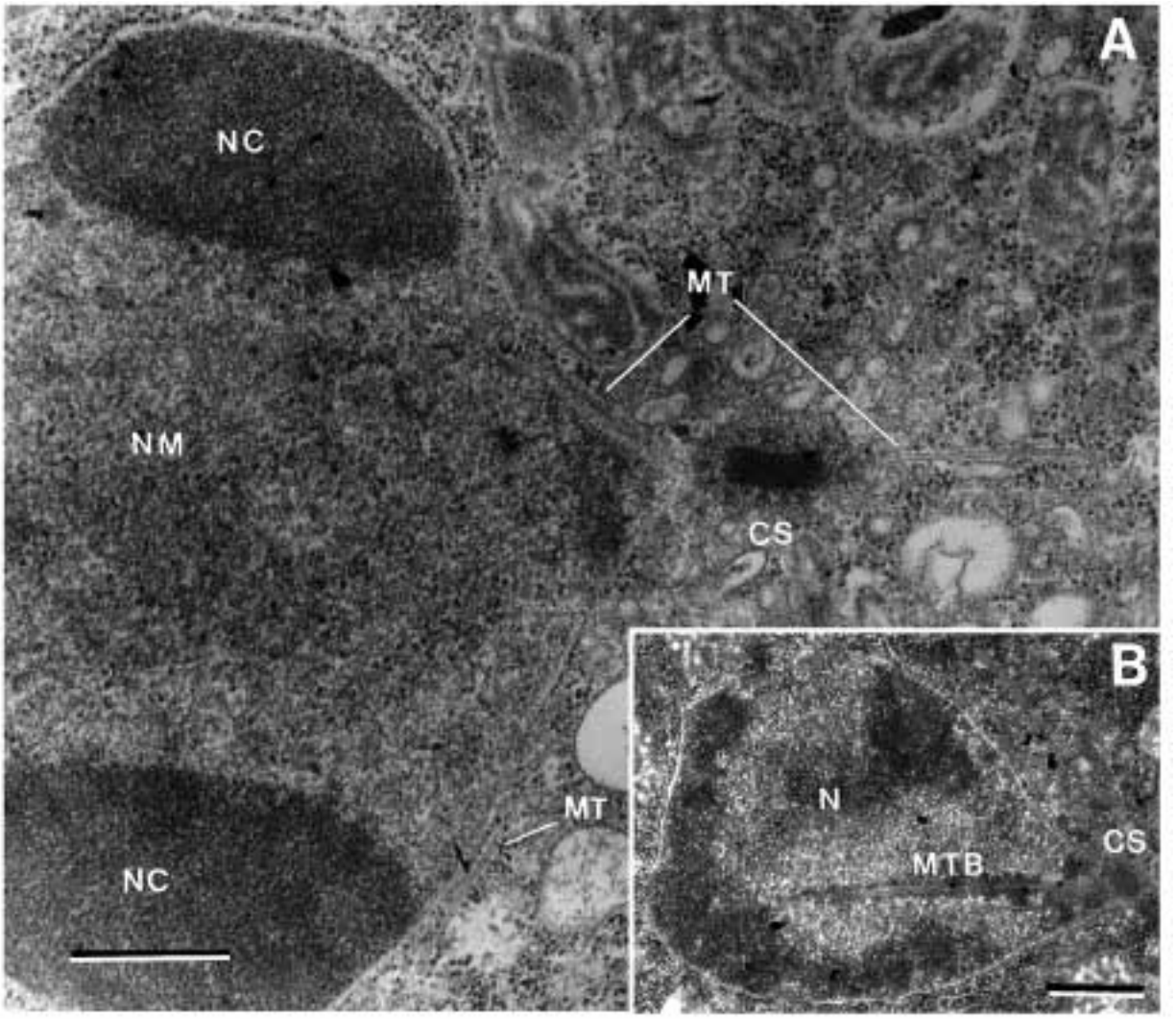

Fig. 6. Electron micrographs of sections through the boundary between centrosome and nucleus. (A) Association of the centrosome with a tipped extension of the nuclear membrane in an interphase cell. (B) An intranuclear bundle of microtubules connected to the centrosome, as seen in fluorescence images of post-mitotic cells. CS, centrosome; N, nucleus; NC, nuclear caps (nucleoli); NM, nuclear matrix; MT, microtubules; MTB, microtubule bundle. Bars, 0.5 μm.

movement of the centrosome and nucleus apply. When the direction of movement abruptly changed, this fluorescent microtubule bundle was elastically bent in a way suggestive of the nucleus being carried by the centrosome in a piggyback manner and dragged against the resistance of the cytoplasm (arrowheads in Fig. 7B).

Guiding microtubules and force transmission to centrosomes in interphase cells

Interphase cells contain long microtubules that span the entire intracellular space and are often bent at the cell periphery. These microtubules are flexible, as indicated by waves of bending that travel along their length. The strongly compressed cell shown in Fig. 8 gives an impression of the forces involved in moving the centrosome, and illustrates how changes in the direction are linked to the switch from one guiding microtubule to another. Two microtubules were drawn as a bundle over the nucleus (Fig. 8, 0- to 37-second frames). Thereafter, the centrosome was pressed against the nucleus, thus deforming it into a heart-shaped body (Fig. 8, 37- to 68-second frames). Subsequently, these guiding microtubules relaxed after their detachment from the cell cortex, and another microtubule took over the guiding role, connecting the centrosome to the left side of the cell cortex (Fig. 8, 100- and 110-second frames). This microtubule became sharply bent at its cortical attachment site. Its terminal portion was oriented parallel to the cell surface, and seemed to increase in length during the translocation of the centrosome towards the cortex (Fig. 8, 171- and 175-second frames). From five consecutive images an average radius of curvature of 1.4 μm was calculated for this microtubule at its site of bending.

These results, suggesting a function of microtubules in centrosome motility, accord with the inefficiency of butanedione monoxime (BDM) to block the motility of centrosomes. BDM inhibits the ATPase activity of myosins (Cramer and Mitchison, 1995). Centrosome movement was

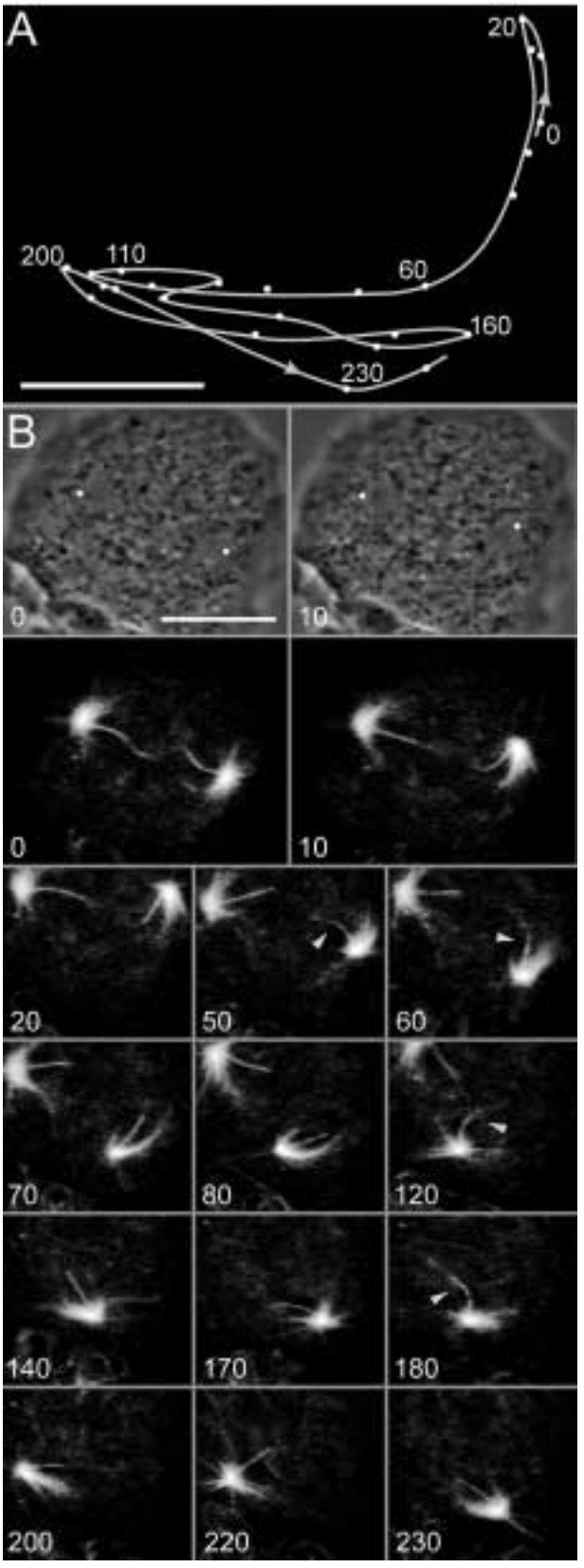

Fig. 7. Saltatory centrosome movement in a post-mitotic myosin II-null cell and co-transport of the nucleus. (A) Centrosome track indicating variations in the speed of movement and abrupt changes in direction, often by nearly 180°. Centrosome positions were determined at 10 second intervals of scanning. Numbers indicate seconds after beginning of the sequence. (B) Phase-contrast (top panels) and confocal fluorescence images of GFP-α-tubulin (all other panels) illustrating movement of the centrosome whose track is shown in A. In the phase-contrast images, centrosome positions taken from the corresponding fluorescence images are indicated by white dots. The centrosome on the right is the tracked one. Between 210 and 230 seconds, centrosome movement was accelerated from 0.04 to 0.7 μm per second. Elastic bending of the intranuclear rod of microtubules is marked by arrowheads. Guiding microtubules in front of the centrosome are recognizable at 80 and 230 seconds, which correspond to phases of high-speed motility. Seconds on the frames are consistent with those in A. Bars, 5 μm (A), 10 μm (B).

still observed in cells treated with 50 mM BDM. This was the highest concentration applicable, since at 100 mM BDM obviously unspecific effects were observed, including the dissociation of microtubules.

DISCUSSION

Cytokinesis versus traction-mediated cytofission

The fluorescence imaging of GFP-tagged α-tubulin in combination with phase-contrast microscopy made it possible continually to monitor the interplay between microtubules and the cell cortex in wild-type and myosin II-null cells. The GFP-labelled microtubules reflected all changes in the mitotic apparatus that have previously been recognized in cells that are free of any GFP-tag (Neujahr et al., 1997a).

The analysis of mitosis revealed that multinucleate myosin II-null cells were not only capable of initiating the formation of furrows as shown before (Neujahr et al., 1997a), but also to complete cleavage (Figs 2-4). Like the cleavage furrows that are formed during cytokinesis in uninucleate cells, those formed in the multinucleate myosin II-null cells are concave with a rounded contour and sharp demarkation from the polar regions of the cells (Fig. 2A). Movement of these ruffling regions is usually negligible during cytokinesis and alone would never separate the daughter cells. This is exemplified by the multinucleate myosin II-null cell shown in Fig. 3, where the front positions of two incipient daughter cells remain almost unchanged during progression of the cleavage furrows (cells on top and on the right of the 170- to 560-second frames). It is typical of the final step of cytokinesis in *Dictyostelium* that the cleavage products are held together by a confined strand of cytoplasm, which ultimately disrupts when the daughter cells move apart. This is seen in wild-type as well as uninucleate and multinucleate myosin II-null cells (Figs 1A,B, 2A,B, 3B, 4A).

Cytokinesis, i.e. mitotic cleavage in multinucleate myosin II-null cells as described here, is clearly distinguishable from traction-mediated cytofission, a process not linked to mitosis (Spudich, 1989). Cytofission is essentially due to the activity of a leading edge, which by its migration draws a portion out of a multinucleate cell until only a thin thread of cytoplasm connects this portion with the main cell body (Fig. 3 in Warrick

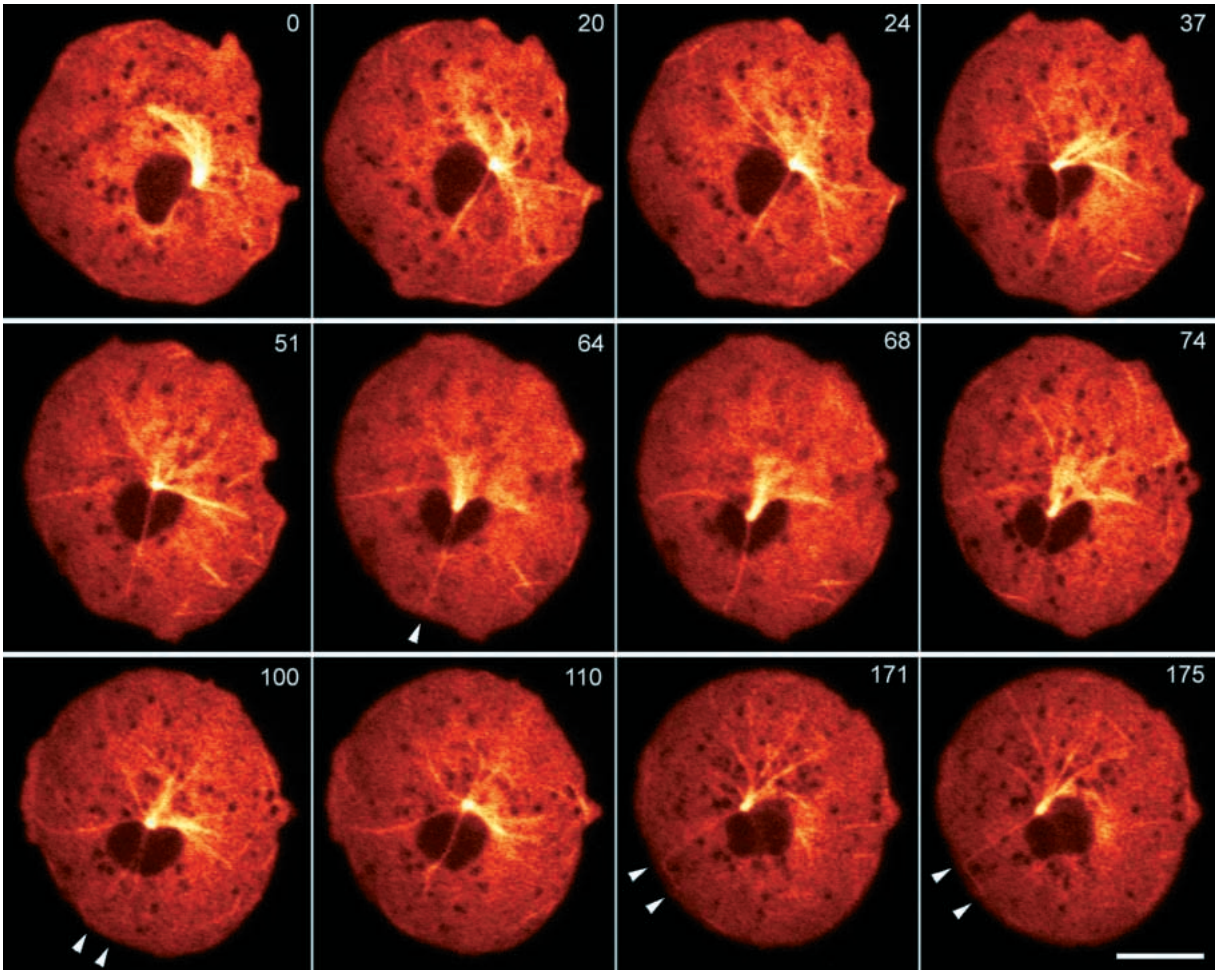

Fig. 8. Guiding microtubules connecting the centrosome with the cortex in an interphase cell. This sequence shows fluorescence images of GFP-α-tubulin in a strongly compressed wild-type cell. The dark area in the middle is the nucleus; dark spots are mostly mitochondria. To make delicate structures more easily distinguishable, fluorescence intensities are colour coded from dark red (low intensity) to bright yellow (high intensity). In the first frame most of the microtubules form a tail behind the centrosome, some of them being bent when the centrosome is turning towards the left (20-second frame). Microtubules laterally associated with the nucleus are drawn over the nucleus. After their attachment to the cell cortex (arrowhead at 64 seconds), the centrosome is translocated towards the bottom, thereby deforming the nucleus. At 74 seconds two guiding microtubules are discernible, which at 100 seconds have lost contact with the cortex (arrowhead). The actual guiding microtubule in the last two frames is sharply bent. The site of its association with the cell cortex and its apparent end are indicated by arrowheads. Bar, 10 μm.

and Spudich, 1987). The cytoplasmic bridge may eventually break, but in our experience it often retracts and the extension is eventually drawn back into the main body of the cell.

Features of multinucleate cells relevant to models of cytokinesis

Current models of cytokinesis are based on findings which indicated that a cleavage furrow is distinguished from the polar regions by its high contractile activity and stiffness (Swann and Mitchison, 1953; Wolpert, 1966; White and Borisy, 1983; Harris and Gewalt, 1989; Rappaport, 1996; Burton and Taylor, 1997; He and Dembo, 1997; Oegema and Mitchison, 1997). The centrosomes, or the asters of microtubules surrounding them, are generally considered to be the major sources of signals that make the furrow distinct from the poles. Emphasis is either placed on a relaxation of the cortical regions on top of the asters (White and Borisy, 1983), or on the induction of contractility at the midzone of the cell (Devore et al., 1989).

In the multinucleate myosin II-null cells studied, cell-surface ruffling is linked to docking of the centrosomes to the cell cortex, and the formation of cleavage furrows is restricted to areas separating the asters of microtubules from each other (Figs 2A, 3B, 4A). In sea urchin blastomeres (Rappaport, 1986) as well as in *Dictyostelium* (Niewöhner et al., 1997) and the related genus *Polysphondylium* (Roos and Cattelan-Kohler, 1989), the spindle is dispensable for the formation of a cleavage furrow. Accordingly, gaps between asters that are not supported by a spindle can give rise to a furrow on the surface of multinucleate cells (Fig. 3). The system controlling cleavage is probably less complicated in *Dictyostelium* than in mammalian cells, where signals derived from the spindle are involved in the initiation of a furrow (Cao and Wang, 1996; Wheatley et al., 1997).

Our data strongly suggest that the asters exert a local influence on the cell cortex, stimulating ruffling and suppressing cleavage furrow formation. The suppression of furrowing is evident in large multinucleate myosin II-null cells, in which the surface area to volume ratio is lower than in uninucleate cells (Fig. 2C). The limitation of surface area results in a denser packing of the centrosomes in the cortical layer, which will not leave enough space between them for the initiation of furrows. These results are consistent with the view that there is a general increase of contractile activity in the course of mitosis (Hara et al., 1980; Schroeder, 1981) and, at the sites of their docking, the asters antagonize this activity.

The sharp demarkation recognized in multinucleate myosin II-null cells between the furrows and the ruffling portions of the cell surface is a general feature of cytokinesis. White and Borisy (1983) make allowance for this sharp boundary by assuming mobile contractile elements that accumulate in the furrow region.

In the multinucleate myosin II-null cells, cleavage furrows reach contour lengths that exceed by severalfold cleavage furrows typical of uninucleate cells (Figs 2-4). Since the centrosomes are moving away from their initial sites of docking while the furrows proceed to incise the cell body, the asters cannot exert a continued influence on the furrow region (Fig. 3). Progression of cleavage furrows is, therefore, a self-sustained process, which indicates that the signals required for initiating a furrow are no longer needed for its maintenance and expansion. This self-sustained progression of cleavage furrows is a tenet of the polar relaxation concept of White and Borisy (1983). According to this model, the influence of asters is limited to the initiation of a furrow. He and Dembo (1997) have taken self-sustained progression of a furrow into account by modeling contraction as a slightly autocatalytic process.

Striking aberrations from a bilateral symmetry in the formation and progression of cleavage furrows are characteristic of cytokinesis in the multinucleate myosin II-null cells. Tripartite cleavage occurs at sites where a furrow comes in contact with two other furrows (Fig. 2A). The formation of unilateral furrows (Fig. 2B) relates mitotic cleavage in *D. discoideum* to cytokinesis in amphibian embryogenesis, where this phenomenon has previously been analysed (Hara, 1971). The formation of unilateral furrows is inconsistent with any hypothesis that requires a closed contractile ring for cytokinesis, and suggests that contractile elements are continuously recruited to, and eliminated from, the progressing furrow.

Which proteins specify a cleavage furrow and how is the force for its constriction produced?

Differential activation of members of the ras family of small GTPases along a dividing cell might be responsible for the induction of ruffling at the poles and its suppression in the furrow. RacE (Larochelle et al., 1996), rasG (Tuxworth et al., 1997) and two homologs of GTPase-activating proteins (Faix and Dittrich, 1996; Adachi et al., 1997), are implicated in cytokinesis of *Dictyostelium* cells. By contact of the GTP-rich caps of microtubules with the cell cortex a rac isoform may be activated that induces ruffling. The finding that tubulin binds in vitro specifically to the GTP-bound form of Rac1 (Best et al., 1996) supports of this possibility.

Neither in uninucleate nor in multinucleate cells is myosin II essential for the formation of a cleavage furrow (Neujahr et al., 1997a; this paper). However, myosin II increases the reliability and speed of cytokinesis in *Dictyostelium* cells anchored to a substrate (Neujahr et al., 1997a) and is indispensable for the cleavage of cells in suspension (DeLozanne and Spudich, 1987; Knecht and Loomis, 1987). Myosin II is typically accumulated on both sides of a cleavage furrow, suggesting that it plays a role in stabilizing the furrow and restricting its position to the midzone of the cell (Neujahr et al., 1997b). The spreading of cleavage furrows over a major portion of the cell surface, as illustrated in Figs 2B, 3B and 4A, is possibly due to the lack of myosin II.

If myosin II is not essential for cytokinesis, which proteins endow the furrow with the mechanical properties necessary for cleavage? *Dictyostelium* cells contain more than 12 unconventional myosins. Some of these might support contractility of the cleavage furrow, although only myosin II is known to form bipolar filaments. Pair-wise elimination of myosins I has caused little, if any, impairment of cytokinesis (Jung et al., 1996; Novak et al., 1995). Strong impairment of cytokinesis has been obtained, however, by the knock-out of two non-motor proteins in *Dictyostelium*, the F-actin bundling and crosslinking proteins cortexillin I and II (Faix et al., 1996). This effect of the loss of non-motor proteins indicates that a local increase in stiffness can replace the function of myosin II in furrow formation. The recent model of He and Dembo (1997) is in agreement with the possibility that proteins other than myosin II may contribute to constriction by increasing the cortical stiffness in the furrow region relative to the poles of a dividing cell.

Guiding microtubules and motor proteins involved in centrosome motility

A common denominator in the interaction of mitotic and interphase centrosomes with the cell cortex is the involvement of microtubules that span from the centrosome to the cell cortex. These guiding microtubules point into the actual direction of centrosome movement, while the majority of microtubules are dragged behind and bent when the centrosome changes direction. The finding that forces responsible for movement of the nuclei apply on the centrosomes (Fig. 7B) accords with previous data on early *Drosophila* embryogenesis, where forces acting on the centrosomes mediate the migration of nuclei to the cell cortex (Raff and Glover, 1989).

Are microtubule- or actin-based motor proteins engaged in moving the centrosome in myosin II-null cells? Unconventional myosins might be involved; however, inability of the myosin-ATPase inhibitor BDM (Cramer and Mitchison, 1995) to block centrosome motility does not support this possibility. Our data are consistent with the view that centrosomes are moved by microtubule-based motors that are anchored to the plasma membrane or bound to the cortical network of actin filaments. Dynein, or other minus-end directed motors, may pull on the guiding microtubules in front of the centrosome, and plus-end directed kinesins may push on the trailing microtubules behind the organelle. Although our data do not exclude a contribution of kinesins in the movement of centrosomes, they are consistent with a primary role of a minus-end directed motor, probably cytoplasmic dynein.

The measured velocities of centrosome movement of

between 0.2 and 0.7 μm per second are comparable to the speed of 0.9 μm per second obtained for dynein-driven microtubule motility in vitro (Koonce and McIntosh, 1990). Motility of centrosome-microtubule complexes with similar speed has been found in leukocytes after TPA-induced centrosome splitting (Euteneuter and Schliwa, 1985). The finding that this motility is inhibited by cytochalasin D provides support for an anchorage of microtubule-based motors to the actin cytoskeleton.

In yeast evidence has been provided that the spindle pole body is pulled towards the bud, and the spindle is orientated, by a dynein-driven process (Carminati and Stearns, 1997; Shaw et al., 1997). These movements are associated with the depolymerization of microtubules that contact the cell cortex at their plus end. In *Dictyostelium*, the anaphase movement of asters towards the cell periphery may be based in a similar manner on the shortening of microtubules (Fig. 5C). As in anaphase cells of yeast, the aster microtubules interacting with the cell cortex display dynamic instability in *Dictyostelium*. The microtubule pattern appears to change even one order of magnitude faster in *Dictyostelium* than in yeast, if Fig. 5A,C,D of this paper is compared with Fig. 3 by Shaw et al. (1997). This accelerated microtubule re-organization is in accord with the fast passage of *Dictyostelium* cells through ana- and telophase (Fig. 1A).

It is hard to reconcile that the long-term circulation of centrosomes shown in Fig. 4B is based on an alternation of attachment and shortening of guiding microtubules, as is the centrosome movement in yeast. Furthermore, microtubules bent at their cortical attachment site indicate that, at least in interphase cells, microtubules are not immediately depolymerized at their plus end when they contact the cell cortex (Fig. 8). We prefer, therefore, a model of centrosome motility in *Dictyostelium* that is based on microtubule gliding. By imposing force on microtubules, minus-end directed motor proteins fixed to the cell cortex may mediate both the saltatory and circulatory centrosome movement observed in the present study (Figs 4B, 7). Direction will change in a saltatory fashion when a guiding microtubule is replaced by another one. The comet-like circulatory movement of a centrosome, together with a bunch of trailing microtubules, can be explained by continuous traction exerted on the minus end of a guiding microtubule (Fig. 9).

D. discoideum contains a single gene encoding dynein heavy chain (Koonce et al., 1992). The dynein is localized in the cytoplasm and strongly enriched at the centrosome and nucleus (Koonce and McIntosh, 1990). Its activity can be reduced by the dominant negative effect of an N-terminally truncated fragment. Overexpression of this fragment impairs the interaction of interphase microtubules with the cell cortex, leading to whorls of microtubules that are connected to the centrosome (Koonce and Samsó, 1996). Probably these whorls, observed in fixed cells, circulate in living cells as the comet-like arrays in small myosin II-null cells do (Fig. 4B). In normal interphase cells, multiple microtubules pointing in different directions will keep the centrosome in balance at a distance from the cell surface. In unusually small cells or in cells with reduced dynein activity, this balance is obviously not achieved, causing the centrosome to circulate close to the cell surface.

A final point to be discussed is the apparent flexibility of microtubules observed in vivo. This flexibility contrasts to physical measurements based on thermal fluctuations, which indicated that microtubules polymerized in vitro are stiff, with a persistence length of about 5 mm (Gittes et al., 1993; Mickey and Howard, 1995). MAPs even increase the flexural rigidity of microtubules (Felgner et al., 1996). Bending of the spindle (Fig. 2C) and kinks in cytoplasmic microtubules close to their cortical attachment sites (Fig. 8, 171- and 175-second frames) suggest a mechanism in vivo for the relaxation of microtubules. The observed bending radius of less than 2 μm parallels findings in vitro that led Amos and Amos (1991) to propose that dynein can distort the microtubule lattice in a non-elastic fashion. Dynein molecules attached to the cell cortex may twist a guiding microtubule and irreversibly alter its structure, as suggested by the coiling of microtubules after their detachment from the cell cortex (Fig. 8, 110-second frame).

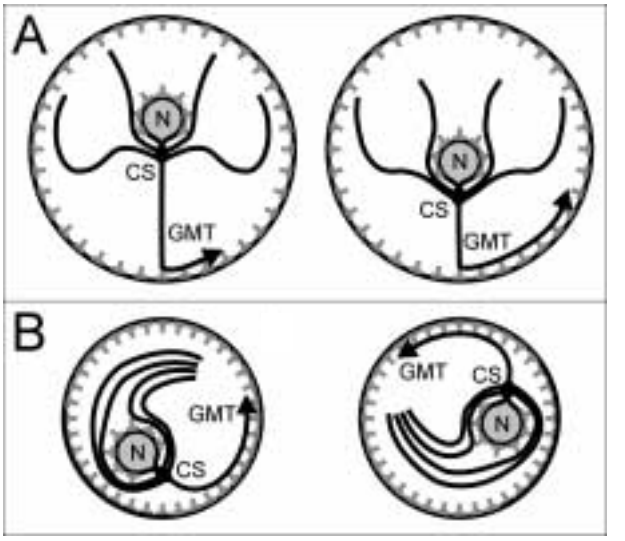

Fig. 9. Schemes of the proposed driving of centrosomes by dynein. The diagrams are based on the circular centrosome movement shown in Fig. 4B, the saltatory movement analysed in Fig. 7, and the behaviour of guiding microtubules demonstrated in Fig. 8. One or a few of the microtubules emanating from a centrosome are supposed to bind to dynein that is attached to the cell cortex, probably via dynactin (Carminati and Stearns, 1997). These guiding microtubules are assumed to draw the centrosome by the minus-end directed motor activity of dynein towards their cortical site of attachment. The assumption that dynein is the motor involved is based on previous studies by Koonce and McIntosh (1990) and Koonce and Samsó (1996). However, dynein can be replaced in the scheme by any other minus-end directed microtubule motor. CS, centrosome; GMT, guiding microtubule; N, nucleus. Decoration of the cell cortex and nucleus with dynein is indicated by spikes.

Prospects

Giant multinucleate cells, as used here in combination with a GFP-tag on microtubules and centrosomes, provide a tool with which to search for proteins involved in cytokinesis. The myosin II-deficient cells have the advantage that any contribution of this motor protein to cytokinesis is excluded. By mutational analysis, factors may be identified that mediate the docking of mitotic complexes to the cell cortex or act as motor or adaptor proteins in microtubule-mediated centrosome

motility. The large, sharply confined furrows of multinucleate myosin II-null cells will help to localize proteins other than myosin II to the cleavage furrow. Among the candidates are cortexillin I and II, which are actin-bundling proteins shown to mechanically stabilize the cell cortex (Simson et al., 1998) and to be required for normal cytokinesis (Faix et al., 1996).

Mechanisms similar to those reported here may specify spindle position in early embryogenesis (Hyman and White, 1987) and neurogenesis (Chenn and McConnell, 1995), where orientation of the spindle determines cell fate. Evidence suggests that in early cleavage stages of *Caenorhabditis elegans* the spindles are positioned by microtubules, which transmit traction from the cell cortex onto centrosomes (Hyman, 1989). Analysis of the regulation of dynein or other microtubule motors in the cell cortex may therefore unravel centrosome-based activities that contribute to the generation of cell and tissue architecture. The crucial question to be answered in centrosome positioning is how a microtubule is turned into a guiding one, and how this role comes to a halt.

We thank Chris Clougherty and Gerard Marriott for intense discussions and reading the manuscript, and him and Chun-Lin Lu for the α-tubulin clone. The AX2-derived myosin II-null strain is a gift of Dietmar Manstein. The pDBsr vector was provided by Annette Erdmann and the pDEXRH vector by Jan Faix. Christina Heizer provided expert assistance. Grants were supplied by the Deutsche Forschungsgemeinschaft (SFB 266, project D7) and the Fonds der Chemischen Industrie.

REFERENCES

Adachi, H., Takahashi, Y., Hasebe, T., Shirouzu, M., Yokoyama, S. and Sutoh, K. (1997). *Dictyostelium* IQGAP-related protein specifically involved in the completion of cytokinesis. *J. Cell Biol.* **137**, 891-898.

Amos, L. A. and Amos, W. B. (1991). The bending of sliding microtubules imaged by confocal light microscopy and negative stain electron microscopy. *J. Cell Sci.* **suppl. 14**, 95-101.

Best, A., Ahmed, S., Kozma, R. and Lim, L. (1996). The Ras-related GTPase Rac1 binds tubulin. *J. Biol. Chem.* **271**, 3756-3762.

Burton, K. and Taylor, D. L. (1997). Traction forces of cytokinesis measured with optically modified elastic substrata. *Nature* **385**, 450-454.

Cao, L.-G. and Wang, Y.-L. (1996). Signals from the spindle midzone are required for the stimulation of cytokinesis in cultured epithelial cells. *Mol. Biol. Cell* **7**, 225-232.

Carminati, J. L. and Stearns, T. (1997). Microtubules orient the mitotic spindle in yeast through dynein-dependent interactions with the cell cortex. *J. Cell Biol.* **138**, 629-641.

Chenn, A. and McConnell, S. K. (1995). Cleavage orientation and the asymmetric inheritance of Notch 1 immunoreactivity in mammalian neurogenesis. *Cell* **82**, 631-641.

Conrad, G. W. and Schroeder, T. E. (eds) (1990). Cytokinesis: mechanisms of furrow formation during cell division. *Ann. NY Acad. Sci.* **582**, 327 pp.

Cramer, L. P. and Mitchison, T. J. (1995). Myosin is involved in postmitotic cell spreading. *J. Cell Biol.* **131**, 179-189.

DeLozanne, A. and Spudich, J. A. (1987). Disruption of the *Dictyostelium* myosin heavy chain gene by homologous recombination. *Science* **236**, 1086-1091.

Devore, J. J., Conrad, G. W. and Rappaport, R. (1989). A model for astral stimulation of cytokinesis in animal cells. *J. Cell Biol.* **109**, 2225-2232.

Euteneuer, U. and Schliwa, M. (1985). Evidence for an involvement of actin in the positioning and motility of centrosomes. *J. Cell Biol.* **101**, 96-103.

Faix, J. and Dittrich, W. (1996). DGAP1, a homologue of rasGTPase activating proteins that controls growth, cytokinesis and development in *Dictyostelium discoideum*. *FEBS Lett.* **394**, 251-257.

Faix, J., Steinmetz, M., Boves, H., Kammerer, R. A., Lottspeich, F., Mintert, U., Murphy, J., Stock, A., Aebi, U. and Gerisch, G. (1996). Cortexillins, major determinants of cell shape and size, are actin-bundling proteins with a parallel coiled-coil tail. *Cell* **86**, 631-642.

Felgner, H., Frank, R. and Schliwa, M. (1996). Flexural rigidity of microtubules measured with the use of optical tweezers. *J. Cell Sci.* **109**, 509-516.

Gittes, F., Mickey, B., Nettleton, J. and Howard, J. (1993). Flexural rigidity of microtubules and actin filaments measured from thermal fluctuations in shape. *J. Cell Biol.* **120**, 923-934.

Hara, K. (1971). Cinematographic observation of surface contraction waves (SCW) during early cleavage of *Axolotl* eggs. *Wilhelm Roux' Arch. Entw. mech. Org.* **167**, 183-186.

Hara, K., Tydeman, P. and Kirschner, M. (1980). A cytoplasmic clock with the same period as the division cycle in *Xenopus* eggs. *Proc. Nat. Acad. Sci USA* **77**, 462-466.

Harris, A. K. and Gewalt, S. L. (1989). Simulation testing of mechanisms for inducing the formation of the contractile ring in cytokinesis. *J. Cell Biol.* **109**, 2215-2223.

He, X. and Dembo, M. (1997). On the mechanics of the first cleavage division of the sea urchin egg. *Exp. Cell Res.* **233**, 252-273.

Heim, R. and Tsien, R. Y. (1996). Engineering green fluorescent protein for improved brightness, longer wavelength and fluorescence resonance energy transfer. *Curr. Biol.* **6**, 178-182.

Hyman, A. A. (1989). Centrosome movement in the early divisions of *Caenorhabditis elegans*: A cortical site determining centrosome position. *J. Cell Biol.* **109**, 1185-1193.

Hyman, A. A. and White, J. G. (1987). Determination of cell division axes in the early embryogenesis of *Caenorhabditis elegans*. *J. Cell Biol.* **105**, 2123-2135.

Jung, G., Wu, X. and Hammer III, J. A. (1996). *Dictyostelium* mutants lacking multiple classic myosin I isoforms reveal combinations of shared and distinct functions. *J. Cell Biol.* **133**, 305-323.

Knecht, D. A. and Loomis, W. F. (1987). Antisense RNA inactivation of myosin heavy chain gene expression in *Dictyostelium discoideum. Science* **236**, 1081-1086.

Koonce, M. P., Grissom, P. M. and McIntosh, J. R. (1992). Dynein from *Dictyostelium:* primary structure comparisons between a cytoplasmic motor enzyme and flagellar dynein. *J. Cell Biol.* **119**, 1597-1604.

Koonce, M. P. and McIntosh, J. R. (1990). Identification and immunolocalization of cytoplasmic dynein in *Dictyostelium*. *Cell Mot. Cytoskel.* **15**, 51-62.

Koonce, M. P. and Samsó, M. (1996). Overexpression of cytoplasmic dynein's globular head causes a collapse of the interphase microtubule network in *Dictyostelium*. *Mol. Biol. Cell* **7**, 935-948.

Larochelle, D. A., Vithalani, K. K. and DeLozanne, A. (1996). A novel member of the *rho* family of small GTP-binding proteins is specifically required for cytokinesis. *J. Cell Biol.* **133**, 1321-1329.

Manstein, D. J., Titus, M. A., DeLozanne, A. and Spudich, J. A. (1989). Gene replacement in *Dictyostelium*: generation of myosin null mutants. *EMBO J.* **8**, 923-932.

McIntosh, J. R., Roos, U.-P., Neighbors, B. and McDonald, K. L. (1985). Architecture of the microtubule component of mitotic spindles from *Dictyostelium discoideum*. *J. Cell Sci.* **75**, 93-129.

Mickey, B. and Howard, J. (1995). Rigidity of microtubules is increased by stabilizing agents. *J. Cell Biol.* **130**, 909-917.

Moens, P. B. (1976). Spindle and kinetochore morphology of *Dictyostelium discoideum*. *J. Cell Biol.* **68**, 113-122.

Neujahr, R., Heizer, C. and Gerisch, G. (1997a). Myosin II-independent processes in mitotic cells of *Dictyostelium discoideum*: redistribution of the nuclei, re-arrangement of the actin system and formation of the cleavage furrow. *J. Cell Sci.* **110**, 123-137.

Neujahr, R., Heizer, C., Albrecht, R., Ecke, M., Schwartz, J.-M., Weber, I. and Gerisch, G. (1997b). Three-dimensional patterns and redistribution of myosin II and actin in mitotic *Dictyostelium* cells. *J. Cell Biol.***139**, 1793-1804.

Niewöhner, J., Weber, I., Maniak, M., Müller-Taubenberger, A. and Gerisch. G. (1997). Talin-null cells of *Dictyostelium* are strongly defective in adhesion to particle and substrate surfaces and slightly impaired in cytokinesis. *J. Cell Biol.* **138**, 349-361.

Novak, K. D., Peterson, M. D., Reedy, M. C. and Titus, M. A. (1995). *Dictyostelium* myosin I double mutants exhibit conditional defects in pinocytosis. *J. Cell Biol.* **131**, 1205-1221.

Oegema, K. and Mitchison, T. J. (1997). Rappaport rules: cleavage furrow induction in animal cells. *Proc. Nat. Acad. Sci.* USA **94**, 4817-4820.

Raff, J. W. and Glover, D. M. (1989). Centrosomes, and not nuclei, initiate pole cell formation in *Drosophila* embryos. *Cell* **57**, 611-619.

Rappaport, R. (1961). Experiments concerning the cleavage stimulus in sand dollar eggs. *J. Exp. Zool.* **148**, 81-89.

Rappaport, R. (1986). Establishment of the mechanism of cytokinesis in animal cells. *Intern. Rev. Cytol.* **105**, 245-281.

Rappaport, R. (1996). Cytokinesis in animal cells. 386 pp. Cambridge University Press, Cambridge, UK.

Roos, U.-P. and Cattelan-Kohler, H. (1989). Formation and dynamics of the mitotic spindle in the cellular slime mold *Polysphondylium violaceum*. *Eur. J. Cell Biol.* **50**, 56-65.

Shaw, S. L.,Yeh, E., Maddox, P., Salmon, E. D. and Bloom, K. (1997). Astral microtubule dynamics in yeast: a microtubule-based searching mechanism for spindle orientation and nuclear migration into the bud. *J. Cell Biol.* **139**, 985-994.

Schejter, E. D. and Wieschaus, E. (1993). Functional elements of the cytoskeleton in the early *Drosophila* embryo. *Annu. Rev. Cell Biol.* **9**, 67-99.

Schroeder, T. E. (1981). The origin of cleavage forces in dividing eggs. A mechanism in two steps. *Exp. Cell Res.* **134**, 231-240.

Simson, R., Wallraff, E., Faix, J., Niewöhner, J., Gerisch, G. and Sackmann, E. (1998). Membrane bending modulus and adhesion energy of wild-type and mutant cells of *Dictyostelium* lacking talin or cortexillins. *Biophys. J.* **74**, 514-522.

Spudich, J. A. (1989). In pursuit of myosin function. *Cell Regulation* **1**, 1-11.

Straight, A. F., Marshall, W. F., Sedat, J. W. and Murray, A. W. (1997). Mitosis in living budding yeast: anaphase A but no metaphase plate. *Science* **277**, 574-578.

Swann, M. M. and Mitchison, J. M. (1953). Cleavage of sea-urchin eggs in colchicine. *J. exp. Biol.* **30**, 506-513.

Trivinos-Lagos, L., Ohmachi, T., Albrightson, C., Burns, R. G., Ennis, H. L. and Chisholm, R. L. (1993). The highly divergent α- and β-tubulins from *Dictyostelium discoideum* are encoded by single genes. *J. Cell Sci.* **105**, 903-911.

Tuxworth, R. I., Cheetham, J. L., Machesky, L. M., Spiegelmann, G. B., Weeks, G. and Insall, R. H. (1997). *Dictyostelium* RasG is required for normal motility and cytokinesis, but not growth. *J. Cell Biol.* **138**, 605-614.

Warrick, H. M. and Spudich, J. A. (1987). Myosin structure and function in cell motility. *Annu. Rev. Cell Biol.* **3**, 379-421.

Wheatley, S. P., Hinchcliffe, E. H., Glotzer, M., Hyman, A. A., Sluter, G. and Wang, Y.-L. (1997). CDK1 inactivation regulates anaphase spindle dynamics and cytokinesis in vivo. *J. Cell Biol.* **138**, 385-393.

White, J. G. and Borisy, G. G. (1983). On the mechanisms of cytokinesis in animal cells. *J. Theor. Biol.* **101**, 289-316.

Wolpert, L. (1966). The mechanical properties of the membrane of the sea urchin egg during cleavage. *Exp. Cell Res.* **41**, 385-396.

Yumura, S., Mori, H. and Fukui, Y. (1984). Localization of actin and myosin for the study of ameboid movement in *Dictyostelium* using improved immunofluorescence. *J. Cell Biol.* **99**, 894-899.